ELSEVIER

Polymer 42 (2001) 1515–1523

polymer

www.elsevier.nl/locate/polymer

Intriguing morphology transformation due to the macromolecular rearrangement of poly(L-lactide)-*block*-poly(oxyethylene): from core–shell nanoparticles to band structures via fragments of unimolecular size

T. Fujiwara, M. Miyamoto, Y. Kimura*, S. Sakurai

Department of Polymer Science and Engineering, Kyoto Institute of Technology, Matsugasaki, Sakyo-ku, Kyoto 606-8585, Japan

Received 11 April 2000; received in revised form 9 June 2000; accepted 12 June 2000

Abstract

We report on anomalous structural organization from core–shell nanoparticles of a hydrophobic/hydrophilic diblock copolymer consisting of semi-crystalline poly(L-lactide) (PLLA) and poly(oxyethylene) (PEG). The copolymer was synthesized and suspended in an aqueous medium to prepare its core–shell particles. The resultant nanoparticles were spread on a germanium substrate to trace the particle aggregation by atomic force microscopy (AFM) and FT-IR spectroscopy. On the substrate surface, the core–shell particles were found to change their shape into disks, with the PLLA blocks being slightly crystallized. When heated to 60°C, these disk-like aggregations burst into small fragments and then turned to band structures. On the other hand, any ordered structure was not observed when a solution of PLLA-PEG was cast on the surface. In the freeze-dried sample of the suspension, it was found that a lamellar microphase-separated structure was created with crystallization of the PLLA blocks by annealing. The lamella thickness analyzed by the small- and wide-angle X-ray scatterings of this sample was reasonably correlated with the width of the band structures formed on the germanium surface. It is therefore concluded that the formation of the regular band structures can be guided by both the phase separation and crystallization behaviors of the semicrystalline block chains of PLLA-PEG.

Keywords: Poly(L-lactide); Poly(oxyethylene); Nanoparticle

1. Introduction

Various types of microphase-separated structures have been observed in the solid state of block copolymers, where two or more polymer chains are covalently linked at the molecular level [1]. Most of the copolymers extensively studied are made of non-crystalline segments, and the driving force for their phase separation is mainly ascribed to the repulsive force between the block segments. Another class of block copolymers, consisting of semi-crystalline segments, can also form a microphase-separated structure. The morphological behavior in the latter case is very different from that of the amorphous block copolymers because of segment crystallization in addition to micro phase separation [2–5]. In spite of the importance of crystalline block copolymers, few analyses have been done on the structure of the latter or its formation process because of its complexity. Recently, much attention has been paid to the block copolymers involving poly-L-lactide (PLLA) and poly(oxyethylene) (PEG) as hydrophobic and hydrophilic blocks, respectively, because of their wide applications in the biomedical field. For example, versatile drug-delivery systems [6,7] and temperature-dependent sol–gel systems [8] have been developed with these PLLA-PEG copolymers having different block lengths. In addition to their importance in applications, the PLLA-PEG copolymers inherent dual nature as crystalline and amphiphilic copolymers provide a great opportunity to investigate the structural organization of semicrystalline block copolymers.

In the present study, a typical A-B diblock copolymer comprising PLLA (A) and PEG (B) was prepared, and its core–shell nanoparticles were made in an aqueous medium. The resultant particle dispersion was then developed on a germanium substrate to follow the particle aggregation on surface by atomic force microscopy (AFM) and fourier-transform infrared spectroscopy (FT-IR). Additionally, the particles were coagulated into a bulk material in order to analyze the solid state structure by small- and wide-angle X-ray scattering techniques. These analyses revealed the dynamic process of macromolecular dissociation, aggregation and ordering, promoting the understanding of the

* Corresponding author. Tel.: +81-75-724-7804; fax: +81-75-712-3956.
E-mail address: ykimura@ipc.kit.ac.jp (Y. Kimura).

0032-3861/01/$ - see front matter
PII: S0032-3861(00)00454-7

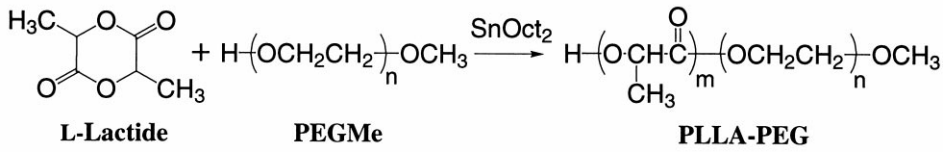

Scheme 1.

mechanism of anomalous structural organization from the core–shell nanoparticles reported previously [9] and in the present paper.

2. Experimental

2.1. Materials

L-Lactide was supplied by Purac Biochem (Netherlands) and purified by recrystallization from ethyl acetate. Monomethoxy-terminated poly(oxyethylene) (PEGMe) with a number average molecular weight (M_n) of 5000 Da and a polydispersity of M_w/M_n (weight/number average molecular weight) = 1.05 was purchased from Aldrich Chemical Co., Inc., and lyophilized from benzene before use. Stannous 4-ethylhexanoate ($Sn(Oct)_2$) was supplied by Nacalai Tesque Co. (Japan) and distilled under high vacuum. It was dissolved in distilled toluene to have a concentration of 0.1 g/ml. Tetrahydrofuran (THF), chloroform, and diethyl ether were commercially supplied and distilled before use. A transparent polymer film (thickness: 250 μm) of PLLA (M_w: 140,000, Da $M_w/M_n = 1.9$) was supplied by Mitsui Chemical Corp. (Japan).

2.2. Measurements

500 MHz ^{1}H NMR spectra were measured on a Bruker ARX-500 spectrometer in $CDCl_3$ or D_2O, respectively, containing 0.03 vol% of tetramethylsilane (TMS) or sodium 3-(trimethylsilyl)propanesulfonate (DSS) as the internal reference. Transmission FT-IR spectra were recorded on a JASCO FT/IR-5300 spectrometer in the wavenumber range 4600–400 cm^{-1}. M_n and M_w/M_n were determined by gel-permeation chromatography (GPC). The analyzer was composed of a Shimadzu LC-10A pump, a Shimadzu refractive-index detector, and a Shimadzu C-R7A Chromatopac data processor. A combination of two polystyrene gel columns of Tosoh TSK gel G4000H8 and G2500H8 was used with chloroform as an eluent at 35°C. The molecular weight was calibrated according to polystyrene standards. Dynamic light scattering (DLS) and static light scattering (SLS) were measured on an Otsuka Electronics DLS-7100 instrument, and the data were analyzed according to the cummulant method. Atomic force microscopy (AFM) was conducted on a Digital Instruments Nanoscope-IIIa operated in the tapping mode in air using a silicon cantilever. Wide-angle X-ray scattering (WAXS) was carried out using a Shimadzu GX3 diffractometer operated at 40 kV and 20 mA. Film specimens were exposed to the Cu Kα (λ = 0.154 nm) radiation and the scattering intensity was measured in the Bragg angle 2θ from 10 to 50°. The sample-to-detector distance was 33.7 mm. Small-angle X-ray scattering (SAXS) was conducted using a synchrotron radiation as the X-ray source at the BL-10C beamline in the Photon Factory of the National Organization for High Energy Accelerator, (Tsukuba, Japan). The incident beam was focused with a bent cylindrical mirror and monochromatized with a pair of Si (111) crystals. The wavelength λ of the incident beam was 0.1488 nm. A 1D potion-sensitive proportional counter (PSPC) was used to detect intensities and was set vertically at a position of 1.9 m behind the sample. The measured SAXS data were corrected for the air scattering and the absorption due to the specimen. The data were further corrected for thermal diffuse scattering arising from density fluctuations.

2.3. Polymer synthesis

The diblock copolymer poly(L-lactide)-*block*-poly(oxyethylene)-monomethyl ether (PLLA-PEG) was prepared according to the methods reported by Langer and the present authors [6,10], in which the ring-opening polymerization of L-lactide was driven from the hydroxy tail of PEGMe (Scheme 1: synthetic route of PLLA-PEG). Ten grams of L-lactide and 10 g of PEGMe were charged into a 300-ml flask. After the mixture was dried in vacuo for 3 h, 0.73 ml of the toluene solution of $Sn(Oct)_2$ (10 mol% relative to PEGMe) was added to the mixture under a nitrogen atomosphere. The mixture was heated and stirred at 120°C for 7 h. At the end of the polymerization the product was cooled, dissolved in 100 ml of chloroform, and poured into a large excess of diethyl ether for reprecipitation of the polymeric product. The precipitate was filtered and vacuum-dried at 60°C overnight to obtain the copolymer as powders in 96% yield. Fig. 1a shows its ^{1}H NMR spectrum in $CDCl_3$; δ 1.56–1.6 (d, CH_3 for PLLA), 3.37 (s, OCH_3 for PEGMe), 3.6–3.7 (m, CH_2CH_2O for PEG), 4.3–4.4 (m, $COOCH_2$ connecting PEG with PLLA), and 5.1–5.2 (q, CH for PLLA). Detection of a singlet signal due to the methoxy group and a multiplet signal of the -$COOCH_2$- group at the connection point suggest that one PLLA sequence has propagated from the hydroxy tail of PEGMe. From the lactate/oxyethylene unit ratio, the weight ratio of PLLA/PEG was calculated to be 52/48, which was similar to the feed ratio of L-lactide/PEG = 50/50. The M_n value was 10,500 Da calculated from the ^{1}H NMR spectrum. The M_n

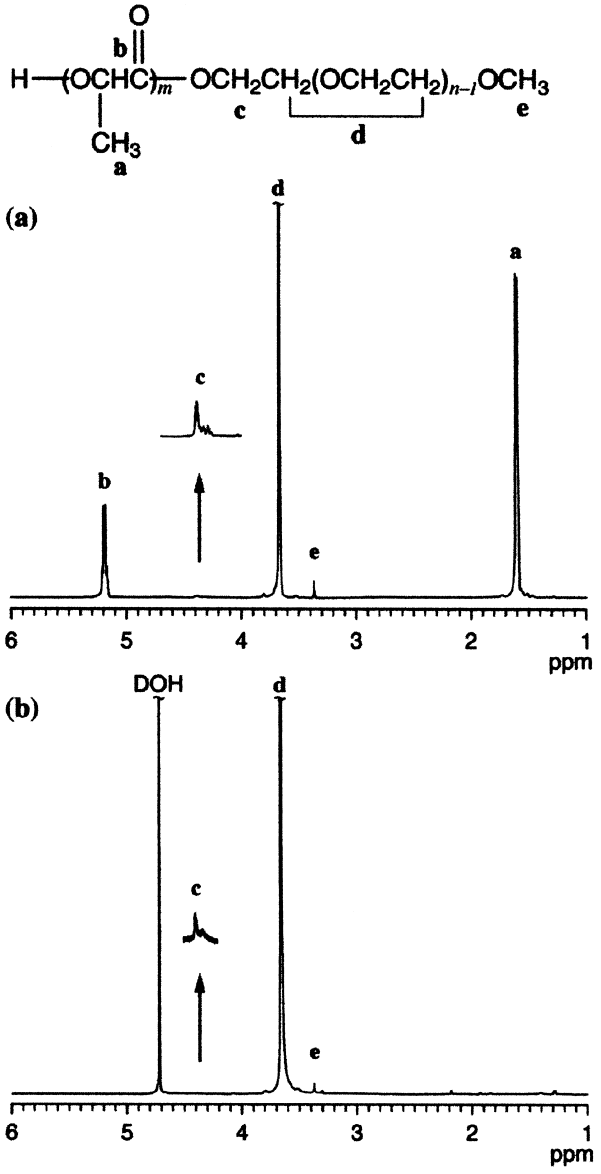

Fig. 1. The 500 MHz ^{1}H NMR spectra of PLLA-PEG in: (a) solution state in $CDCl_3$; and (b) suspension state in D_2O.

value as revealed by GPC was ca. 12,000 Da with a narrow polydispersity of $M_w/M_n = 1.14$. Two endothermic peaks were detected at 46–57°C and 140–160°C in the DSC curve of this PLLA-PEG, corresponding to the crystal fusions of the PEG and PLLA chains, respectively. Both peak temperatures were slightly lower than the melting points of their corresponding homopolymers (PEG: 64°C and PLLA: 175°C). The melting point depletion may be ascribed to imperfect crystallization in microdomain space and in turn may suggest microphase separation in the melt state of this diblock copolymer.

The PLLA-PEG thus obtained as powders is hereafter referred to as "powder sample". It was melt-quenched, and annealed at 120°C for 10 min to obtain an "annealed powder sample".

2.4. Preparation of particle suspensions

A solution of 0.1 g of PLLA-PEG in 5.0 ml of THF was added dropwise into 50 ml of water at 0°C with an ultrasonic wave applied from a dipped sonic probe to obtain a suspension of PLLA-PEG. Then, THF was evaporated from the suspension under reduced pressure at 10°C, and the aqueous suspension was filtered through a 5-μm-pore filter (Fuji, FM-500). The particle concentration in the finally obtained suspension was 0.2 wt%. This suspension was lyophilized. The PLLA-PEG obtained as dried particles is referred to as "particle sample". It was melt-quenched and annealed at 120°C for 10 min to obtain an "annealed particle sample".

2.5. Casting of the particles

The suspension thus prepared was cast on a surface-polished Ge plate (10×10 mm^2) and dried in air at 4°C to prepare a thin film of the PLLA-PEG particles. The thickness of the resultant particle film was estimated to be ca. 400 nm. This film was then annealed at 60°C for 2 h, to study the structural organization.

2.6. Estimation of degree of crystallinity of PLLA

To consider a mechanism of the structural organization from PLLA-PEG nanoparticles, it is important to figure out change in degree of crystallinity of PLLA upon the structural organization. However, quantitative estimation of the crystallinity is impossible by the ordinary WAXS method, because of trace amount of the samples. To overcome the difficulty, we utilized transmission FT-IR measurement for a thin layered sample, which is cast onto the Ge plate where the Ge plate is transparent. Note that the sample cast onto the Ge plate is used for AFM observations. Here, the combined method of FT-IR with WAXS is presented, in order to quantitatively estimate the crystallinity of PLLA for samples in trace amount.

A PLLA film supplied was hot-pressed at 190°C and quenched in liquid nitrogen to obtain an amorphous film sample of PLLA. This film was annealed at 110°C for 2 h to obtain a semi-crystalline sample. Fig. 2a and b show typical WAXS profiles of the amorphous and semi-crystalline films, respectively. The former shows an amorphous halo, whereas the latter shows two sharp diffraction peaks. The peak at $2\theta = 17°$ is attributed to reflection from (200) or (110) plane and that observed at $2\theta = 19°$ from (203) or (113) plane of the α-crystals of PLLA, which consist of 10/3 helical chains [11,12]. Here, the areas of the crystal peaks (I_c) and the amorphous halo (I_a) in the curve (b) were evaluated by the peak-resolving method, and the apparent degree of crystallinity (X) of PLLA was estimated by the

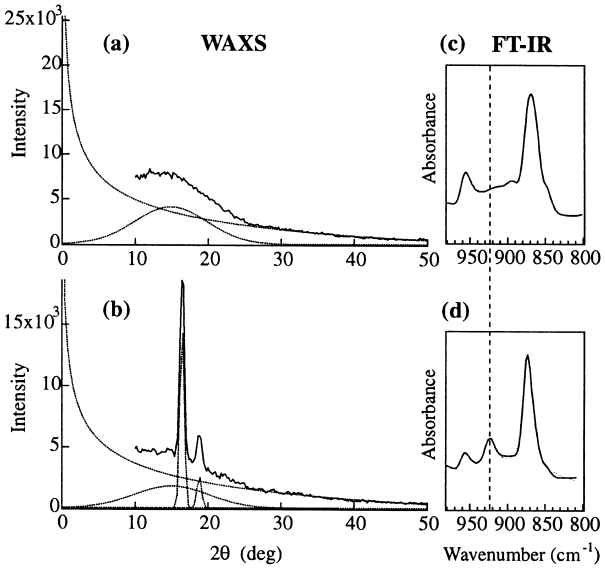

Fig. 2. WAXS profiles and FT-IR spectra of: (a, c) amorphous (melt-quenched) and (b, d) semi-crystalline (annealed at 110°C for 2 h) PLLA films. All the data were obtained at room temperature.

following equation [13]:

$$X = \frac{\int_{2\theta=10^\circ}^{2\theta=50^\circ} I_c s^2 \, ds}{\int_{2\theta=10^\circ}^{2\theta=50^\circ} (I_c + I_a) s^2 \, ds}, \qquad s = \frac{2\sin\theta}{\lambda}, \tag{1}$$

where λ and θ are wavelengths of the X-ray and half the scattering angle, respectively, and s denotes the magnitude of the scattering vector. The X value obtained for the annealed PLLA film was 0.40.

Fig. 2c and d show typical transmission FT-IR spectra of the amorphous and semi-crystalline PLLA films, respectively. Peak assignment can be done by referring to the literature [14–16]. It is noted here that the absorption peak at 922 cm^{-1} is a crystal band characteristic of the helical backbone of PLLA, and that the neighboring band at 957 cm^{-1}, which decreases with crystallization, is attributed to the CH_3 rocking modes. Since both bands were overlapped, the real absorbance of the crystal band was evaluated by the peak-resolving method. The relative absorbance R_c of the crystal band with respect to the carbonyl band at 1759 cm^{-1} can be correlated to X as follows:

$$R_c = A_{922}/A_{1759} = cX, \tag{2}$$

where A_{922} and A_{1759} are absorbances at the wavenumbers shown by the subscripts, and c is a constant. The carbonyl band was used as the internal reference, because its absorbance was independent of the crystallinity and simply proportional to the film thickness. The R_c value thus calculated for the annealed sample was 0.0173. Since the X value determined for this sample by WAXS was 0.40, the value of c was evaluated to be 0.0435. Thus, the crystallinity of PLLA samples in trace amount can be estimated quantitatively by FT-IR measurements through the relationship given by Eq. (2).

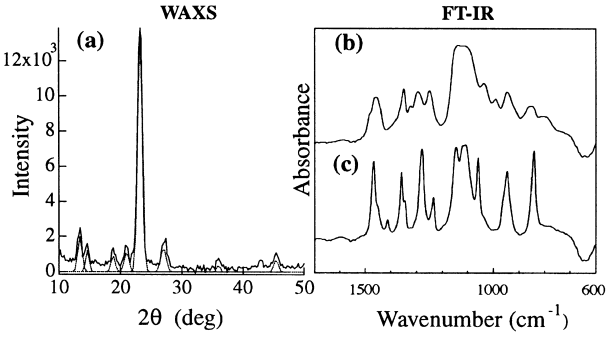

Fig. 3. A typical WAXS profile of: (a) PEGMe, and FT-IR spectra of: (b) amorphous (melt) and (c) semi-crystalline (quenched at room temperature) PEGMe. All the data were obtained at room temperature.

2.7. Crystallization of PEG blocks

Fig. 3a shows a typical WAXS profile of PEGMe (M_n = 5000 Da). The sharp peak at $2\theta = 23^\circ$ is attributed to the reflection of the (112) plane of the monoclinic PEG crystal lattice consisting of 7/2 helical chains. Since it shows almost no amorphous halo, PEGMe is found to be highly crystallized with a degree of crystallinity close to unity at room temperature.

The FT-IR spectra of PEGMe in melt and solid states were quite different from each other. When the molten PEGMe was cooled, many band-shifts were observed suggesting immediate crystallization. Judging from the band-shifts, the crystallization was completed within 30 s at room temperature.

3. Results and discussion

3.1. Characterization of nanoparticles

The suspension of the PLLA-PEG diblock copolymer was prepared by mixing a THF solution of the copolymer into an aqueous medium with ultrasonic wave applied. Although the method employed in the present study is different from that reported by other researchers [6–8], the particle formation of the copolymer has been established. Fig. 1b shows the ^1H NMR spectrum of a similar suspension prepared in D_2O. Different from Fig. 1a, only the PEGMe signals are shown because the aggregation of the PLLA blocks in the core prevents their signal from appearing. When a small portion of 2 N NaOH was added to this sample, the signals of sodium lactate showed up in the spectrum. These facts support the idea that the copolymer formed the core–shell type particles in an aqueous medium comprising the hydrophobic PLLA blocks in the core and the hydrophilic PEG blocks in the shell. The detection of the

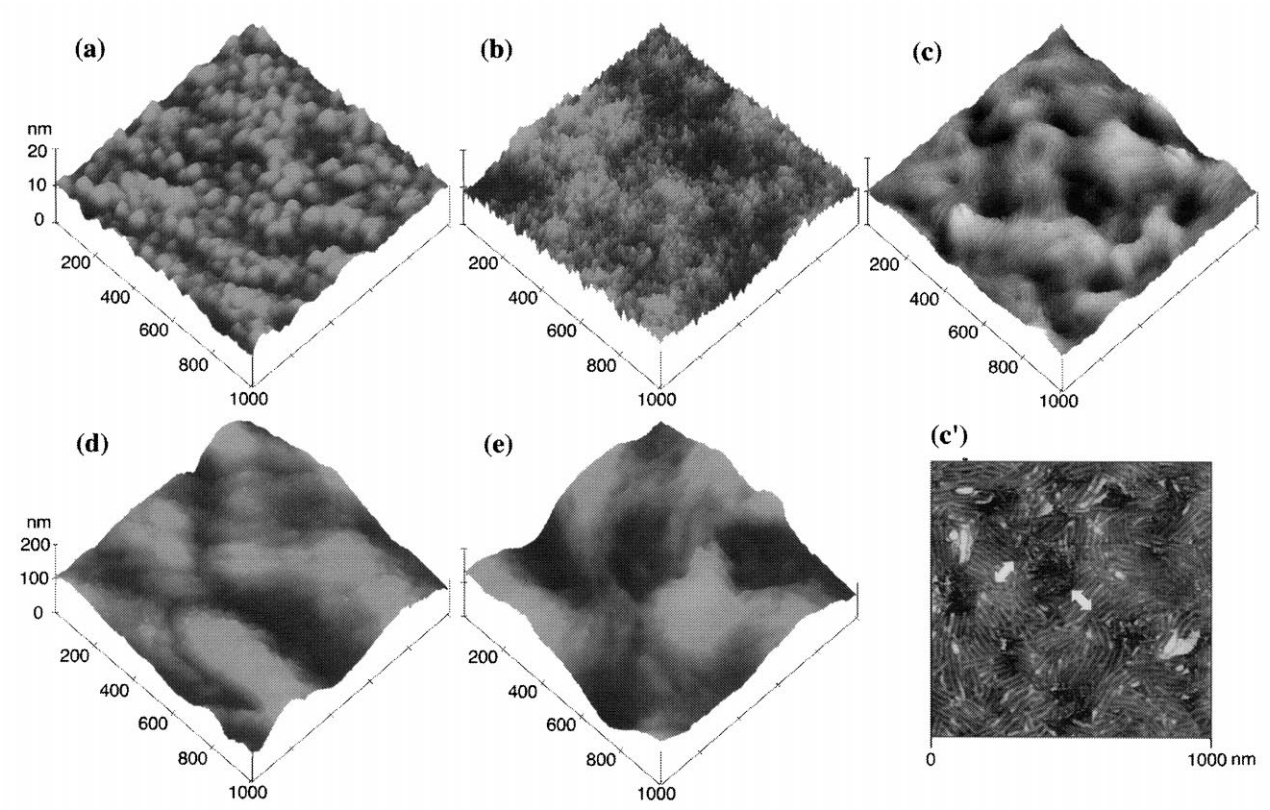

Fig. 4. AFM topological images of PLLA-PEG samples spread on a germanium surface. Samples prepared from the 0.2 wt% aqueous suspension: (a) as-cast at 4°C, (b) as-heated to 60°C, (c) after annealing at 60°C for 2 h, and (c′) the phase image corresponding to the topological image of (c). Samples prepared from the 0.2 wt% THF solution: (d) as-cast at 4°C and (e) after annealing at 60°C for 2 h.

small methoxy signal **e** in Fig. 1b may indicate that the terminal methoxy groups of the PEG blocks are localized in a surface of the shell to have high mobility.

The suspension of the copolymer particle was analyzed by DLS and SLS. The average hydrodynamic diameter of the particles calculated by the cumulant method was 90 nm in the suspension containing 0.2 wt% of the particles. The apparent molecular weight of the nanoparticles was determined to be 1×10^7 Da by SLS. From this value, the average aggregation number of the block copolymer was calculated to be ca. 1×10^3 per particle.

3.2. Aggregation behavior of PLLA-PEG on a substrate surface

The suspension of PLLA-PEG (0.2 wt%) was cast on a Ge substrate and air-dried at 4°C. Fig. 4a shows a typical AFM image of the particle film on the Ge surface. Here, a large number of particles with similar nanometer-size agglomerate closely, to cover the whole surface of the substrate. As verified by the contour of a cross-section, the shape of the particles is discoid, having an average diameter of 30–50 nm and a thickness of 5–10 nm. Therefore, the spherical core–shell particles in the suspension shrank into the smaller disks with evaporation of water during the casting on the substrate. These morphological change and shrinkage of the particles are reasonable because the density changed from 0.04 g/cm^3 of the original particles in the suspension to ca. 1.0 g/cm^3 of the ordinary organic solids on the surface.

Once this suspension-cast sample was heated to 60°C, the AFM image changed drastically as shown in Fig. 4b. Considerably small fragments having a diameter of 5–10 nm are agglomerated. They also have a discoid shape with a thickness of 2–3 nm. This particle size corresponds reasonably to a unimolecular size. Magnification of one region revealed a feature of particle fragmentation in which a number of small particles are emitted from a central particle with a slightly larger size. The same results were observed on a mica surface, which should be referred to a former paper [9]. These data support fragmentation of the particles.

After further annealing at 60°C for 2 h, the AFM image turned to that shown in Fig. 4c, where a mesh-like pattern is seen. The mesh consists of thin bands of ca. 10 nm in width. The band structures can be more clearly visualized by the 2D phase-image shown in Fig. 4c′ (vide infra.). It is suggested that the small fragments shown in Fig. 4b aggregated into the thin band structures, which were arranged parallel to each other in parts.

The structural organization upon the thermal annealing, mentioned above, can be observed only when the suspension of PLLA-PEG particles were cast on the substrate.

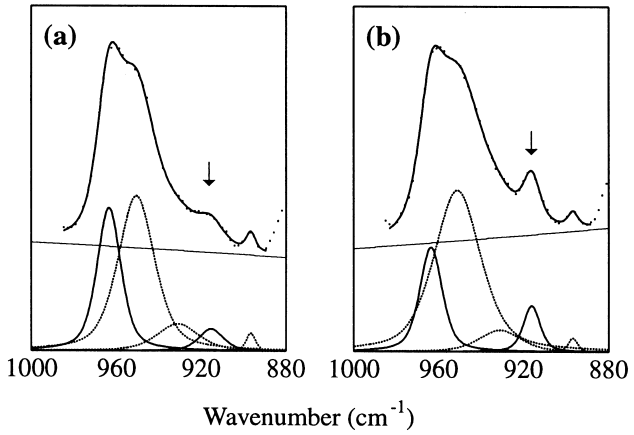

Fig. 5. FT-IR spectra of the PLLA-PEG nanoparticles spread on a germanium surface: (a) as-cast and (b) after annealing at 60°C for 2 h.

When a THF solution of PLLA-PEG (0.2 wt%) was cast on a Ge substrate, no specific structural organization was detected by AFM (Fig. 4d). Even after this solution-cast sample was annealed at 60°C for 2 h, the AFM image (Fig. 4e) showed little change. Moreover, no band structure was observed. When a suspension of PLLA homopolymer and a suspension of a similar block copolymer comprising a racemic poly(DL-lactide) (not crystallizable in nature) were cast in a similar manner, the band structure was not observed, either. These results suggest that the crystallization of the PLLA block chain plays an important role in the formation of band structures. Furthermore, it is expected that the band structures can be formed only through the burst of nanoparticles into small fragments, as seen in Fig. 4b.

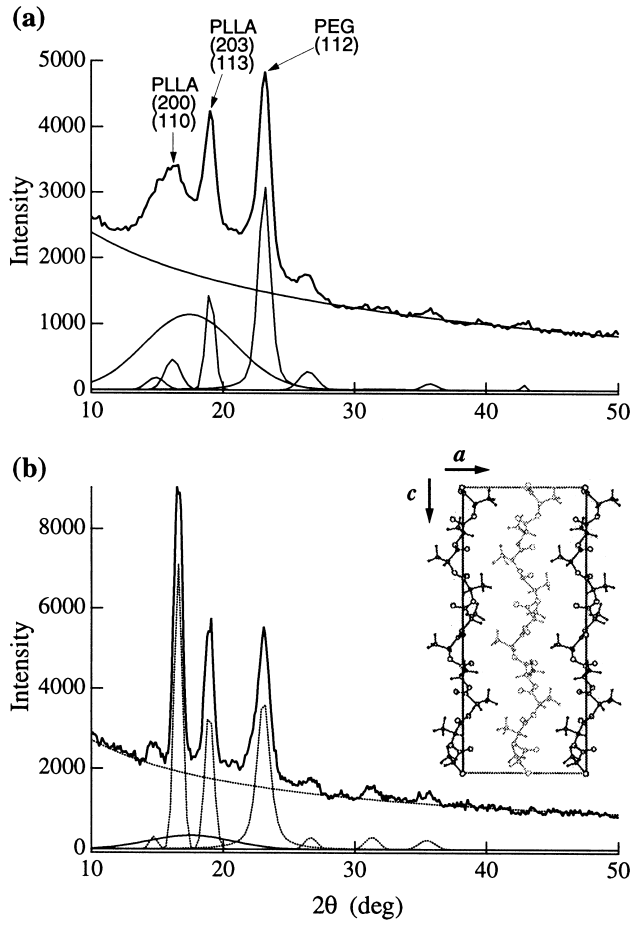

Fig. 6. WAXS profiles of the particle sample of PLLA-PEG: (a) as-lyophilized and (b) after annealing at 120°C for 10 min.

3.3. Change in crystallinity of the particles cast on the substrate upon the annealing

To confirm the significant role of crystallization in the structural organization, the change in crystallinity of the PLLA block chains upon the annealing was examined by the combined method of FT-IR with WAXS. The as-cast and annealed samples of the particles were subjected to the transmission FT-IR measurement, subsequently to the AFM observations (Fig. 4a and c). Fig. 5 shows the spectra observed in the range 1000–880 cm^{-1} with the decomposed individual peaks. The helical band of the PLLA chain appears around 916 cm^{-1}, which is slightly shifted towards the lower wavenumber as compared to that for the PLLA homopolymer. From the relative absorbance $A_{916}/A_{1756}(=R_c)$, the degree of crystallinity of the PLLA blocks was calculated using Eq. (2) to be 0.11 and 0.24, for the (a) as-cast and (b) annealed samples, respectively. Thus, the crystallinity of the PLLA blocks was found to increase upon the annealing. In Fig. 4c the band structures coexist with the small particles whose diameters are less than 10 nm and in which the PLLA chains was not crystallized, so that the crystallinity of the PLLA chains in the band structures is larger than 0.24. On the other hand, the PEG-derived absorption bands were observed only in the crystal regions. This result also supported the fact that the PEG blocks can crystallize very fast.

3.4. Crystallization of the PLLA block chains

In addition to the increase in the crystallinity, it is particularly interesting to examine the growth mechanism of PLLA crystallites upon annealing. For this purpose WAXS measurements are required. However, it is impossible to conduct WAXS measurements on the particle sample in trace amounts. To the first approximation, we assume that the growth mechanism of PLLA crystallites in large amounts of the particle sample is similar and applicable to the case of trace amounts. Thus, we conducted WAXS measurement on large amounts of the particle sample.

Fig. 6a and b show, respectively, the WAXS profile of the particle sample which was freeze-dried and that of its annealed sample (at 120°C for 10 min) with the decomposed individual peaks. Both curves show two intense reflections at $2\theta = 17$ and 19°, which are ascribed to the (200) or (110) plane and the (203) or (113) plane of the PLLA crystal

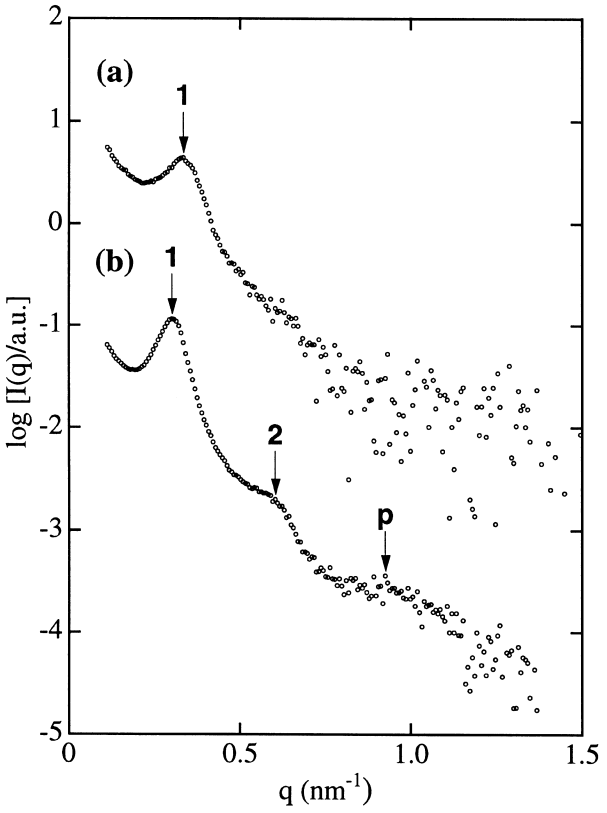

Fig. 7. SAXS profiles of: (a) the powder and (b) particle samples measured at 111–113°C after annealing at 120°C for 10 min.

lattice, respectively, together with another sharp reflection at 23°, which is a diffraction peak from the (112) plane of the PEG crystal lattice. The broad peak located at $2\theta = 18°$ can be assigned to an amorphous halo of the PLLA chains because the crystallinity of PEG is close to unity. As a matter of fact, the (112) reflection for the PEG crystallinity at $2\theta = 23°$ did not increase in its intensity upon the annealing. Peak-resolving enabled us to calculate the degrees of crystallinity of the PLLA block chains in the particle sample and annealed particle sample to be 0.18 and 0.74, respectively. In the annealed sample, a very high crystallinity of the PLLA blocks was attained.

By using Scherrer's equation [17], the average crystallite thickness normal to the (200) or (110) plane and that normal to the (203) or (113) plane of the PLLA crystals were calculated. In the particle sample the thicknesses were 12 and 20 nm, respectively, whereas in the annealed particle sample, the thickness normal to the (200) or (110) plane grew to 22 nm, while that normal to the (203) or (113) plane remained constant. This finding indicates that the crystal growth of the PLLA blocks is 1D in the (200) or (110) direction that is perpendicular to the chain axis of PLLA, as shown by the diagram in the inset of Fig. 6.

The WAXS profiles of the powder sample and the annealed powder sample (at 120°C for 10 min) were similar to those of the particle sample and the annealed particle sample, respectively. Accordingly, the degree of crystallinity of the PLLA blocks were found to be 0.20 and 0.85, respectively.

3.5. Microphase-separated structure of the PLLA-PEG diblock copolymer

The band structures found by AFM (Fig. 4c and c′) remind us of lamellar microphase-separated structures. To confirm, the SAXS measurements were conducted on large amounts of the particle sample, where the assumption similar to the case of the WAXS study was made.

Both the powder and particle samples were melted at 160°C for 10 min in vacuum. After the samples became transparent, they were quenched at room temperature, annealed again at 120°C for 10 min, and then subjected to the SAXS measurement at 112 ± 1°C. The SAXS profiles obtained are shown in Fig. 7. The profile (a) of the powder sample exhibits only a first-order peak, lacking the higher-order peaks which afford an important information of the morphology. The Bragg spacing was calculated to be 19 nm from the q value of the first-order peak through the Bragg's equation ($2\pi/q^*$). Since the PEG blocks are melted while the PLLA blocks are crystallized at 112°C, the crystallites of the PLLA blocks give rise to the contrast for X-rays against the melt phase of the PEG blocks and amorphous phase of the PLLA blocks.

The profile (b) of the particle sample clearly shows the higher-order peaks in addition to the first-order peak. Since the first- and second-order scattering maxima are observed at the relative q-values represented by 1:2, formation of lamellar microdomain structures can be considered. Moreover, the broad peak labeled with **p** is due to so-called particle scattering (contribution of the intra particle interference). The q value of the first-order peak gives interdomain distance ($D \equiv 2\pi/q^*$) of 21 nm while the q value of the particle scattering ($q_\mathbf{p}$) gives the average thickness of lamellar particles (lc) through the relationship reported in the literature ($q_\mathbf{p} lc = 8.76$) of 9.5 nm [18]. The ratio lc/D can be considered to be a volume fraction of the PLLA crystallites in the sample, which leads to 0.45. Since the volume fraction of the PLLA blocks is 0.50 in the PLLA-PEG diblock copolymer, the degree of crystallinity of PLLA blocks can be estimated to be 0.9, which is roughly in accord with the result of WAXS.

Comparing the SAXS results, it can be stated that the particle sample can form the lamellar microdomain structure more easily than the powder sample. The white arrows in the AFM image (Fig. 4c′) indicate the length of 100 nm, in which five bands are involved. This value is well correlated with the lc value estimated above. Therefore, the band structures formed by the annealing of the particles reasonably correspond to these lamellar structures of PLLA-PEG.

3.6. Mechanism of the structural organization

Let us consider a mechanism of the structural organization

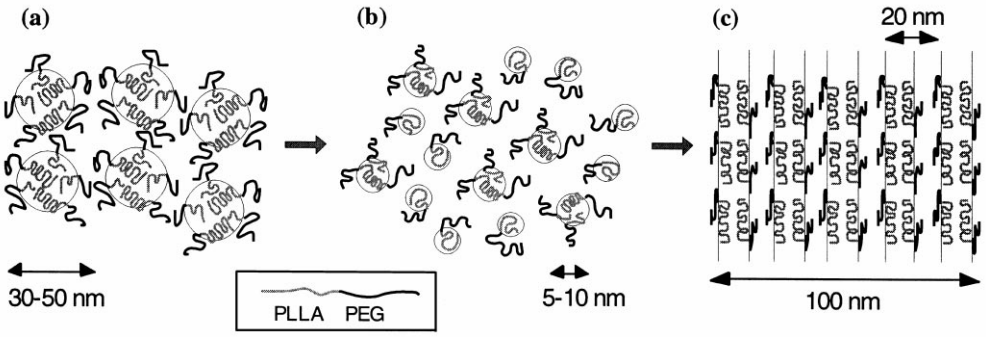

Fig. 8. Schematic illustration of the structural organization for the PLLA-PEG nanoparticles. The PEG and PLLA block chains are represented in black and gray, respectively.

for the particle sample on the basis of the results presented above, especially taking into account the PLLA crystallization and development of the lamellar microdomain structures upon annealing. The whole process of the structural organization for the particle sample is illustrated in Fig. 8. The nanoparticles formed in the aqueous suspension have a stable core–shell structure with a spherical shape, having an average diameter of 90 nm. In these nanoparticles, the PLLA blocks weakly aggregate to have an amorphous state. When cast on a substrate surface, the particles shrink by loss of water and change their morphology into disks having a diameter of 30–50 nm and a thickness of ca. 5–10 nm (Fig. 8a). Although the particles are not so stable and are likely to burst during the drying process, they can retain their particle form in a dense agglomeration state. The crystallization of the PEG blocks may prevent the particles from collapsing. In the core of the particles, the PLLA blocks are only partly crystallized. Judging from the relatively low degree of crystallinity (0.11) of the PLLA blocks, the particles may consist of micro-crystallites, which are not so stable.

These particles in the agglomerate immediately burst into smaller fragments with a diameter of less than 10 nm and a thickness of 1–3 nm, by heat treatment (Fig. 8b). This burst may be caused by the melting of the PEG crystals that have stabilized the particles. The aggregation of the PLLA blocks, being mostly amorphous, can also be relaxed and crystallize above its glass transition temperature (~55°C). Therefore, even the PLLA blocks in a microcrystalline state can be stripped off the particle center.

These fragments re-aggregate into the band structure (Fig. 8c). In this case, the crystal growth of PLLA may govern the organization from (b) to (c). The growth is directed perpendicular to the chain axis of PLLA, i.e. along the *a* or *b* axes, as speculated from the result of WAXS. In Fig. 8c the *c* axis of the PLLA crystallites is considered to orient perpendicularly to the microdomain interface, which enables the PLLA crystallites to grow along the *c* axis, keeping the width of the PLLA lamellar microdomain (in other words, the band structure) constant at ca. 10 nm. According to this model, the length of the PLLA band structures increases with the growth of PLLA crystallites. This is consistent with the findings by AFM shown in Fig. 4c and c′, and previously reported in Ref. [9]. Note that the width of 10 nm for the PLLA band structure and its repeating distance of 20 nm are based on the results of AFM (Fig. 4c and c′) and SAXS (Fig. 7b). Here, the helical macromolecular chains of PLLA can be stacked parallel to the surface in which the crystal growth is guided in one direction to form the band structure. Ding and Liu have recently reported several types of stable aggregates of the nanoparticles of amorphous block copolymers, e.g. polystyrene-*block*-poly(2-cinnamoylethyl methacrylate) [19,20]. The morphology transformation on the mica substrate, however, was quite different from that of the present nanoparticles. This difference is also attributed to the crystalline nature of the blocks of the copolymers.

Generally, amorphous block copolymers form a microphase-separated structure due to the segregation between the blocks [21,22]. On the other hand, block copolymers comprising crystallizable components exhibit complexity in morphological behaviors due to the competition of microphase separation and crystallization. As a matter of fact, in the present powder sample and its solvent-cast sample, the microphase separation proceeds but is not well developed due to the fast crystallization of PEG blocks (Fig. 7a). Nevertheless, the final morphology from the particle sample exhibits highly ordered microdomain structures (Figs. 4c, c′ and 7b). From the particle sample, a non-equilibrium state consisting of the fragments of unimolecular size can be formed by annealing, inducing the crystallization-mediated segment segregation and organization. This process can give a well-organized phase separation structure with a highly ordered lamellar structure. It is particularly interesting to note that the initial nanoparticle form can provide a seed for the well-developed or organized microdomain structures.

4. Conclusions

Core–shell nanoparticles of PLLA-PEG were prepared in an aqueous medium. When the particles were cast and heat-treated on a germanium substrate, the particles burst into

small fragments, which then aggregated into the band structures. Since the crystallinity of the PLLA blocks significantly increased with the band formation (from 0.11 to 0.24), the band structures were considered to be guided by the formation of crystalline lamellae. Any ordered structure was not observed when the same PLLA-PEG was solution-cast on the Ge substrate and treated likewise. SAXS and WAXS analyses of the particle sample, which was melt-quenched and annealed, revealed that a lamellar structure was formed with crystallization of the PLLA blocks, being more regular than that formed in a solid prepared from the powder sample. These results suggest that the initial morphology of the copolymers can control the competition between the segment segregation and crystallization and can govern the final morphology.

Acknowledgements

We acknowledge the support from a Grant-in-aid for Scientific Research on Priority Area, “Sustainable Biodegradable Plastics”, No. 11217210 from the Ministry of Education, Science, Sports and Culture. The SAXS experiments were performed in the Photon Factory with an approved number of 99G232.

References

[1] Araki T, Tran-Cong Q, Shibayama M. Structure and properties of multiphase polymeric materials. New York: Marcel Dekker, 1998.
[2] Wunderlich B. Macromolecular physics, vol. 1. New York: Academic Press, 1973.
[3] Rangarajan P, Register RA, Adamson DH, Fetters LJ, Bras W, Naylor S, Ryan AJ. Macromolecules 1995;28:1422.
[4] Ryan AJ, Hamley IW, Bras W, Bates FS. Macromolecules 1995;35:3479.
[5] Nojima S, Hashizume K, Rohadi A, Sasaki S. Polymer 1997;38:2711–8.
[6] Gref R, Mibamitake Y, Peracchia MT, Trubetskoy V, Torchilin V, Langer R. Science 1994;263:1600.
[7] Hagan SA, Coombes AGA, Garnett MC, Dunn SE, Davies MC, Illum L, Davis SS. Langmuir 1996;12:2153–61.
[8] Jeong B, Bae YH, Lee DS, Kim SW. Nature 1997;388:860–2.
[9] Fujiwara T, Miyamoto M, Kimura Y. Macromolecules 2000;33:2782–5.
[10] Lee CW, Kimura Y. Bull Chem Soc Jpn 1996;69:1787–95.
[11] Kobayashi J, Asahi T, Ichiki M, Okikawa A, Suzuki H, Watanabe T, Fukuda E, Shikinami Y. J Appl Phys 1995;77:2957.
[12] Brizzolara D, Cantow HJ, Diederichs K, Keller E, Domb AJ. Macromolecules 1996;29:191.
[13] Ohkoshi Y, Shirai H, Gotoh Y, Nagura M. SEN’I GAKKAISHI 1999;55:21–27.
[14] Kister G, Cassanas G, Vert M, Pauvert B, Terol AJ. Raman Spectrosc 1995;26:307–11.
[15] Chalmers JM, Mackenzie MW, Willis HA, Edwards HG, Lees JS, Long DA. Spectrochim Acta Part A 1991;47:1667.
[16] Rabolt JF, Moore WH, Krimm S. Macromolecules 1977;10:1065.
[17] Scherrer P. Goettingen Nachr 1918:98.
[18] Koizumi S, Hasegawa H, Hashimoto T. Macromolecules 1994;27:7893.
[19] Ding J, Liu G. Langmuir 1999;15:1738–47.
[20] Ding J, Liu G. Macromolecules 1999;32:8413–20.
[21] Khandpur AK, Macosko CW, Bates FS. J Polym Sci 1995;33:247.
[22] Quiram DJ, Register RA, Marchand GR. Macromolecules 1997;30:4551.